Microbiology (2012), **158**, 2598–2609 **DOI** 10.1099/mic.0.058636-0

The non-classical ArsR-family repressor PyeR (PA4354) modulates biofilm formation in *Pseudomonas aeruginosa*

M. Mac Aogáin,[1]† M. J. Mooij,[1]† R. R. McCarthy,[1] E. Plower,[1] Y. P. Wang,[2] Z. X. Tian,[1,2] A. Dobson,[3,4] J. Morrissey,[3,4] C. Adams[1] and F. O'Gara[1,3,4]

Correspondence
F. O'Gara
f.ogara@ucc.ie

[1]BIOMERIT Research Centre, Department of Microbiology, University College Cork, Cork, Ireland

[2]National Laboratory of Plant Engineering and Protein Genetic Engineering, College of Life Science, Peking University, Beijing, PR China

[3]Marine Biotechnology Centre, Environmental Research Institute, University College Cork, Cork, Ireland

[4]Department of Microbiology, University College Cork, Cork, Ireland

Received 16 February 2012
Revised 30 June 2012
Accepted 16 July 2012

PyeR (PA4354) is a novel member of the ArsR family of transcriptional regulators and modulates biofilm formation in *Pseudomonas aeruginosa.* Characterization of this regulator showed that it has negative autoregulatory properties and binds to a palindromic motif conserved among PyeR orthologues. These characteristics are in line with classical ArsR-family regulators, as is the fact that PyeR is part of an operon structure (*pyeR-pyeM-xenB*). However, PyeR also exhibits some atypical features in comparison with classical members of the ArsR family, as it does not harbour metal-binding motifs and does not appear to be involved in metal perception or resistance. Hence, PyeR belongs to a subgroup of non-classical ArsR-family regulators and is the second ArsR regulator shown to be involved in biofilm formation.

INTRODUCTION

ArsR-family transcriptional repressors are widespread among bacteria and are functionally linked to the detoxification of diverse metals and metalloids (Busenlehner *et al.*, 2003). The metalloregulatory repressor ArsR was the first described member of this large protein family, which was initially identified in *Escherichia coli* as a plasmid-mediated, arsenic-responsive regulator controlling expression of an arsenic resistance operon (San Francisco *et al.*, 1990). ArsR was subsequently characterized at the molecular level, revealing its function as a dimeric autorepressor, which dissociated from its promoter on binding of arsenic or antimony (Shi *et al.*, 1996). Several features of ArsR, including dimerization and metal(loid)-associated de-repression, were found to hold true for diverse ArsR orthologues, such as the cyanobacterial SmtB and CadC of *Staphylococcus aureus*, which regulate metal resistance genes, including metallothionins and metal efflux machinery, in response to toxic metals such as cadmium, zinc and lead (Busenlehner *et al.*, 2003; Huckle *et al.*, 1993). As such, this represents the classical paradigm whereby ArsR regulators allow bacteria to sense and respond to diverse metal(loid)s at the transcriptional level. As both toxic and essential metal(loid)s may be detrimental to bacterial survival, ArsR-family regulators are implicated in the adaptation of bacteria to fluctuating metal(loid) concentrations in their natural environments (Busenlehner *et al.*, 2003; Summers, 2009).

The molecular characterization of metal(loid)-responsive ArsR-family repressors led to the identification of several metal(loid)-binding motifs, which correlate with the specificity of ArsR repressors for diverse di- and multivalent metal(loid)s (Campbell *et al.*, 2007; Harvie *et al.*, 2006; Osman & Cavet, 2010). These motifs can be found among regulators of the ArsR family, thus allowing prediction of the metal(loid)-binding specificities of ArsR-family repressors (Campbell *et al.*, 2007; Harvie *et al.*, 2006). However, several ArsR-family repressors do not harbour obvious metal(loid)-binding motifs, and a number of ArsR repressors do not appear to respond to the presence of metal(loid)s (Barbosa & Benedetti, 2007; Ehira *et al.*, 2010; Gristwood *et al.*, 2011; Gueuné *et al.*, 2008). Moreover, their associated genes have no homology to typical metal resistance genes such as metal reductases, metallothionins and metal efflux pumps, which are generally associated

†These authors contributed equally to this work.

Abbreviations: EMSA, electromobility shift assay; MAST, Motif Alignment and Search Tool; MEME, Multiple Em for Motif Elicitation; MFS, major facilitator superfamily; OYE, old yellow enzyme.

A supplementary table and a supplementary figure are available with the online version of this paper.

with classical ArsR-family repressors (Busenlehner *et al.*, 2003).

Instead, these non-classical ArsR-family repressors, including CyeR of *Corynebacterium glutamicum*, BigR of *Xylella fastidiosa*, PigS of *Serratia* spp. and HlyU of *Vibrio vulnificus*, have been demonstrated to regulate pigment production, toxin production, virulence, sporulation and biofilm formation (Barbosa & Benedetti, 2007; Ellermeier *et al.*, 2006; Gristwood *et al.*, 2011; Liu *et al.*, 2009; Mignot *et al.*, 2003). This highlights the existence of a subgroup of ArsR-family repressors that do not conform to the ArsR metallo-regulatory paradigm.

Many pathogenic bacteria encode ArsR-family repressors in their genomes, including the opportunistic human pathogen *Pseudomonas aeruginosa*, which contains four such genes in its genome (Arunkumar *et al.*, 2009; Cai *et al.*, 1998; Campbell *et al.*, 2007; Liu *et al.*, 2009; Stover *et al.*, 2000; Janga & Pérez-Rueda, 2009; Summers, 2009). These include a classical arsenic-responsive ArsR repressor with homology to ArsR of *E. coli* (PA2277) and three uncharacterized ArsR-family proteins (PAO279, PAO547 and PA4354) (Cai *et al.*, 1998; Stover *et al.*, 2000). The aim of this study was to characterize the novel ArsR-family regulator encoded by *PA4354*, which appears to be a non-classical ArsR-family regulator, as reflected by the fact that PA4354 is encoded within a putative operon with an uncharacterized major facilitator superfamily (MFS) transporter and the old yellow enzyme (OYE)-family reductase XenB (Pak *et al.*, 2000; van Dillewijn *et al.*, 2008). Previously, we showed that PA4354 is directly regulated by the LysR-type transcriptional regulator MexT (Tian *et al.*, 2009a, b). Here we characterize this non-classical PA4354 regulator at the molecular level and investigate its role in mediating key pathogenic traits.

METHODS

Strains and plasmids. The strains and plasmids used in this study are listed in Table 1. All experiments were performed in *P. aeruginosa* strain PAO1, except the biofilm experiment, which was also performed in strain UCBPP-PA14 (PA14). All primers were designed based on the PAO1 genome sequence (NC_002516.2) and are shown in Table 2. All strains were routinely cultured in Luria–Bertani (LB) broth at 37 °C with shaking at 150 r.p.m. Antibiotics were added to cultures where required: for *E. coli*, kanamycin (25 μg ml^{-1}), tetracycline (10 μg ml^{-1}) and chloramphenicol (20 μg ml^{-1}); for *P. aeruginosa*, tetracycline (20–50 μg ml^{-1}), gentamicin (20–50 μg ml^{-1}) and streptomycin (100 μg ml^{-1}).

All plasmids were constructed in *E. coli* S17λpir, which carries the transfer genes of the broad-host-range INcP-type plasmid RP4 integrated into its chromosome. Biparental mating was used to conjugate plasmids into recipient strains. In brief, overnight cultures

Table 1. Bacterial strains and plasmids used in this study

Abbreviations: Ap^r, ampicillin resistance; Km^r, kanamycin resistance; Tc^r, tetracycline resistance; Cm^r, chloramphenicol resistance; Str^r, streptomycin resistance; Gm^r, gentamicin resistance.

Strain or plasmid	Description	Source or reference
Strains		
PAO1	Laboratory strain	
PAO1Δ*PA4354*	*PA4354* deletion mutant	This study
PAO1Δ*PA4355*	*PA4355* deletion mutant	This study
PA14 *PA4354*::*Tm*	Mariner transposon insertion in PA14_56620 (*PA4354*)	Liberati *et al.* (2006)
E. coli DH5α	F$^-$ *ϕ*80 *lacZ*ΔM15 (Δ*lacZYA-argF*) *U169 deoR recA1 endA1 hsdR17*(r_K^-, m_K^-) *phoA supE44 thi-1 gyrA96 relA1 λ*$^-$	Invitrogen
E. coli S17λpir	*pro thi hsdR*$^+$ Tp^r Sm^r; chromosome::RP4-2 Tc::Mu-Kan::Tn*7*/λpir	Simon *et al.* (1983)
BL21-CodonPlus BL21(DE3)-RIPL	Protein expression host	Merck
Plasmids		
pCR2.1-TOPO	Cloning vector, Ap^r, Km^r	Invitrogen
pME6032	pVS1-p15A origin, *lacI*^{q}-P*tac* expression vector, Tc^r	Heeb *et al.* (2000)
pME6032-mexT	pME6032-derived *mexT* expression vector	Tian *et al.* (2009b)
pME6032-PA4354	pME6032-derived *PA4354* expression vector	This study
pET28a	T7 promoter-driven His-tag protein expression vector, Km^r	Novagen
pET28a-PA4354H6C	pET28a-derived C-terminal His_6-tag *PA4354* expression vector	This study
pMP190	*IncQ* origin, low-copy-number *lacZ* fusion vector; Cm^r, Str^r	Spaink *et al.* (1987)
pMP-PA4354p	pMP190-derived *PA4354* promoter-*lacZ* fusion plasmid	Tian *et al.* (2009a)
pMP-PA4354pMa	Mutated version of pMP-PA4354p harbouring mutation in PA4354 repressor binding site	This study
pEX18Tc	*oriT*$^+$, *sacB*$^+$, gene replacement vector, Tc^r	Hoang *et al.* (1998)
pPS856	Gm^r cassette flanked with FRT sequences, Ap^r, Gm^r	Hoang *et al.* (1998)
pFLP3	Inducible Flp recombinase, Tc^r	Hoang *et al.* (1998)

Table 2. Primers used in this study

Primers were designed based on the PAO1 genome sequence (NC_002516.2). Underlined nucleotides indicate incorporated restriction sites.

Primer	Sequence	Incorporated restriction site
***PA4354* overexpression construct pME6032-4354**		
pF54.O	5′-GGAATTCCATGCCACTGGACATCGACG-3′	*Eco*RI
pR54.O	5′-GGGGTACCTGGACTGCGAGGTGGTG-3′	*Kpn*I
***PA4354* deletion mutant**		
p5FD54	5′-CCCAAGCTTCCACCTCCATTGGCAGAGC-3′	*Hin*dIII
p5RD54	5′-CAAGATCCCCAATTCGACTCGAGCATGGCGGTGGTCCGTTG-3′	*Xho*I
p3FD54	5′-GAGCGCTTTTGAAGCTCTCGAGTAAGCAGCACTCGCTTCC-3′	*Xho*I
p3RD54	5′-CGGGATCCAGAAGAACAGGGTGATTTCC-3′	*Bam*HI
p5D54	5′-CGTCGAGCACGTTCAGCACG-3′	
p3D54	5′-GGACCACGTTGACCTGCAGC-3′	
***PA4355* deletion mutant**		
p5FD55	5′-CCCAAGCTTGGGCGAAAGCCTGGAGTTGC-3′	*Hin*dIII
p5RD55	5′-CAGTCGACCATCGGTCGAGCTCCTGG-3′	*Sal*I
p3FD55	5′-GCTCGACCGATGGTCGACTGATCCCCTGTCCGTCTATTC-3′	*Sal*I
p3RD55	5′-CGGGATCCCGTACCGCCGGTATAGAAGGTT-3′	*Eco*RI
p5D55	5′-ACAATTGATAGGTGATTCC-3′	
p3D55	5′-AGGGTCGGATAGTCCAGGTA-3′	
***PA4354-PA4355-xenB* operon structure confirmation**		
pXBrt	5′-TCGGATAGTCCAGGTAGCCT-3′	
pF54-55	5′-AACGAGGAGACCATCCAGGC-3′	
pR54-55	5′-ACGATGAAGATGCCCATCA-3′	
pF55-XB	5′-CGGCAGCGTCATCGACCA-3′	
pR55-XB	5′-AGAGTTGCAGGAAGATGCGC-3′	
Site-directed mutagenesis		
pFsdm54	5′-GTCGCAATCGATCCCCATCGCGTCCCACACCGATAT-3′	
pRsdm54	5′-ATATCGGTGTGGGACGCGATGGGGATCGATTGCGAC-3′	
His-tagged *PA4354* expression construct pET28aPA4354H6C		
pFH54	5′-CATGCCATGGCACTGGACATCGACGAAATC-3′	*Nco*I
pRH54	5′-CCGCTCGAGCAGCTCGTCGCCGAGTTG-3′	*Xho*I
EMSA DNA fragments		
pF54emsa	5′-GATCATCGTCATCAGCCCT-3′	
pR54emsa	5′-AGTGGCATGTGGTCCGTT-3′	
pF81emsa	5′-AGCAAGACCCGTCCGAGAG-3′	
pR81emsa	5′-GATTTCGAAGATTTCGTAAAGGA-3′	

of donor and recipient strains were washed in fresh media and transferred to VSWP 0.025 μm filters (Millipore), which were placed on LB agar to reduce growth and thereby increase conjugation efficiency.

Microcolony formation assay. Artificial sputum medium (ASM) was prepared as described by Sriramulu *et al.* (2005). ASM (1 ml) was inoculated to OD_{600} 0.05 with an overnight culture of *P. aeruginosa* PA14 in 24-well cell-culture plates. IPTG was added at 1 mM for all pME6032-derivative plasmids. Plates were then incubated for 72 h at 37 °C at 150 r.p.m. Three independent biological replicates were performed.

Generation of deletion mutants. Disruption of *PA4354* and *PA4355* was achieved using the gene replacement vector pEX18Tc, as previously described (Tian *et al.*, 2009b). Regions flanking the *PA4354* ORF were amplified using primer sets p5FD54 and p5RD54 (to amplify the *PA4354* 5′ flanking region) and p3FD54 and p3RD54 (to amplify the *PA4354* 3′ flanking region). Chimeric PCR was employed to link the *PA4354* 5′ and 3′ flanking regions. Primers incorporating *Hin*dIII, *Xho*I and *Kpn*I restriction sites were used to generate a 1.8 kb *Hin*dIII–*Kpn*I fragment with a *Xho*I site between the *PA4354* 5′ and 3′ flanking regions into which the excised FRT-containing gentamicin resistance cassette from pPS856 was ligated (Hoang *et al.*, 1998). For generation of the *PA4355* deletion construct, a 5′ flanking region was amplified with primers p5FD55 and p5RD55 and a 3′ flanking region was amplified with primers p3FD55 and p3RD55 to generate a chimeric 1.8 kb *Hin*dIII–*Bam*HI fragment with an intermittent *Sal*I site into which the pPS856 gentamicin cassette was introduced. The pEX18Tc *PA4354* and *PA4355* deletion constructs were transformed into *E. coli* S17λpir and subsequently transferred to PAO1 by conjugation following routine cloning

procedures (Sambrook, 2001). The gentamicin resistance cassette was excised from the PAO1 chromosome using plasmid pFLP3 (Hoang *et al.*, 1998). Successful disruption of target genes was verified in each strain by PCR amplification and DNA sequencing using primers which flanked the deleted *PA4354* (p5D54 and p3D54) or *PA4355* (p5D55 and p3D55) ORFs.

Flow-cell experiments. Bacteria were grown in M63 medium throughout the flow-cell experiments (Sambrook, 2001). Flow-cell chambers with individual channel dimensions of $1 \times 4 \times 40$ mm were used. The flow system was assembled and prepared as described by Pamp *et al.* (2008). The flow chambers were inoculated by injecting 350 µl of overnight culture diluted to OD_{600} 0.001 into each flow channel using a small syringe. After inoculation, the flow channels were left without flow for 1 h, after which medium flow was started using a Watson Marlow 205S peristaltic pump. Mean flow velocity in the flow chambers was 0.2 mm s^{-1}, corresponding to laminar flow with a Reynolds number of 0.02. The flow-cell biofilm system was incubated at 30 °C throughout the experiment. Bacteria were stained using 5 µM SYTO 9 (Invitrogen). Visualization of the biofilm was performed using a Zeiss LSM5 confocal laser scanning microscope equipped with 488 nm laser lines to excite SYTO 9. Three independent biological replicates were performed.

RNA isolation and RT-PCR. RNA was extracted from exponential-phase cultures (OD_{600} of 0.4–0.7) of PAO1 pME6032-mexT using the RNeasy Mini kit (Qiagen). Genomic DNA was removed using RNase-free DNase I (Promega). Using DNA-free RNA samples as template, cDNA was synthesized using AMV reverse transcriptase (Promega) and primer pXBrt, which was complementary to the 3′ region of *xenB*. Co-transcription of the *PA4354-PA4355-xenB* transcript was investigated by PCR using primers which flanked the *PA4354-PA4355* (pF54-55 and pR54-55) and *PA4355-xenB* (pF55-XB and pR55-XB) intergenic regions.

Generation of the PyeR (PA4354) overexpression construct. To generate plasmid pME6032-PA4354, the *PA4354* ORF was amplified using primers pF54.O and pR54.O, which contain incorporated *Eco*RI and *Kpn*I restriction sites, respectively. This fragment was PCR-purified using the QIAquick PCR purification kit (Qiagen), digested and subsequently ligated directly into the pME6032 multiple cloning site downstream of the P*tac* promoter (Heeb *et al.*, 2000). The T4 DNA ligase and all restriction enzymes used in this study were purchased from Roche Applied Sciences.

Analysis of *pyeR* (*PA4354*) promoter activity in response to diverse metals. Induction of *pyeR* in the presence of diverse metals was investigated in a plate-based assay using the *pyeR-lacZ* promoter fusion pMP-PA4354p as a reporter in PAO1. Overnight cultures of PAO1 harbouring pMP-PA4354p were diluted to OD_{600} 0.125, and a bacterial lawn was inoculated onto M9 agar plates containing 0.4 % glucose, 40 µg X-Gal ml^{-1} and 100 µg streptomycin ml^{-1}. Filter paper discs containing metal salts including $ZnSO_4$, V_2SO_4, $MnCl_2$, MoO_4Na_2, $NaAsO_2$, CdCl, $CuSO_4$, K_2TeO_3, $CoCl_2$, $NiCl_2$, $FeCl_3$, $CrCl_3$, $C_8H_4K_2O_{12}Sb_2$, $AgNO_3$, $Pb(NO_3)_2$, $AuCl_3$, $BiNO_3$, Na_2O_3Se and $HgCl_2$ were placed on the centre of each inoculated plate, which was incubated at 37 °C for 16–24 h and examined for induction of expression from the *pyeR-lacZ* reporter fusion, as indicated by an increase in blue pigmentation in the agar resulting from induction of the *lacZ* gene and the breakdown of X-Gal. Concentrations of each of the metal salts are given in Table S1 available with the online version of this paper. The ability of metals, for which induction was observed, to activate expression from the pMP-PA4354p reported fusion was also investigated in PAO1Δ*PA4354* and PAO1Δ*mexT* deletion backgrounds. The diameter of the zones of inhibition around the 6 mm filter paper disc was also measured, to establish inhibitory properties of the metal salts.

***β*-Galactosidase assays.** Expression of *pyeR* (*PA4354*), as measured from pMP190 fusion constructs, was measured by a *β*-galactosidase assay, and promoter activity was calculated and expressed as Miller units (Miller, 1972). Three independent biological replicates were performed.

Site-directed mutagenesis. To introduce mutations into the *PA4354* promoter region, the *PA4354* promoter fragment of pMP-PA4354p was first amplified using previously described primers with incorporated *Xba*I and *Kpn*I restriction sites (Tian *et al.*, 2009a). This fragment was cloned into the pCR2.1-TOPO cloning vector (Invitrogen) and site-specific mutations within the putative PA4354 autoregulatory motif were introduced as described by Fisher & Pei (1997). The site-directed mutations A91C and T92G (relative to the *PA4353* stop codon) were introduced using primers pFsdm54 and pRsdm54 to amplify the entire pCR2.1-TOPO vector harbouring the PA4354 upstream region. The amplified plasmid was transformed into *E. coli* DH5α and the presence of the introduced mutations was verified by DNA sequencing. Once verified, the mutated promoter region was excised and ligated into the *Xba*I and *Kpn*I restriction sites of pMP190 to yield the mutated promoter-*lacZ* fusion construct pMP-PA4354pMa. The ability of PA4354 (as expressed from the pME6032-*PA4354* overexpression construct) to repress activity from the mutated promoter region of pMP-PA4354pMa was assessed in PAO1 by *β*-galactosidase assay (Miller, 1972).

His-tag purification of PyeR (PA4354). The *PA4354* ORF was amplified using primers pFH54 and pRH54 and cloned into the multiple cloning site of pET28a to yield pET28aPA4354H6C, which expressed a C-terminal His-tagged PA4354 protein. This construct was transformed into the *E. coli* expression host strain BL21-CodonPlusBL21(DE3)-RIPL (Merck) and grown at 37 °C with shaking at 150 r.p.m. in 200 ml LB medium containing kanamycin (50 mg ml^{-1}) until OD_{600} 1 was reached. At this point, 1 mM IPTG was added to the culture to induce expression of the His-tagged PA4354 protein. After 4 h, cells were harvested by centrifugation at 5000 ***g*** at 4 °C and stored overnight at −70 °C. Cell pellets were subsequently thawed and resuspended in CelLytic B II buffer (Sigma Aldrich) (10 ml per gram of cell paste) with 5 mg DNase ml^{-1} and 200 µl Protease Inhibitor Cocktail (Sigma) per gram cell paste. Soluble protein was extracted in accordance with the manufacturer's instructions. Protein extract was applied to a Poly-Prep Chromatography Column (Bio-Rad) containing 1 ml of HIS-Select Nickel Affinity Gel (Sigma). The gel was washed with 2 ml sterile deionized water and equilibrated with 5 ml wash buffer (100 mM HEPES, pH 7.5, 10 mM imidazole). Following washing and equilibration steps, the crude protein extract (10 ml) was passed through the column by gravity flow. Protein which bound to the resin was washed twice with 10 ml wash buffer and purified His-tagged PA4354 protein was eluted in wash buffer containing 250 mM imidazole. The homogeneity of the purified PA4354 protein was verified by SDS-PAGE. Purified protein aliquots were either frozen in 20 % (v/v) glycerol at −70 °C or used promptly for electromobility shift assays (EMSAs). Protein concentrations were determined by the Bio-Rad protein assay.

EMSA. Purified PA4354 protein was incubated with an IR-labelled PA4354 promoter fragment generated with DY-682 IR-labelled primers pF54emsa and pR54emsa (Eurofins MWG Operon). EMSA was set up with 20 µl reaction volumes containing varying concentrations of purified PA4354 protein (10–2000 nM) in the presence of 10 fmol of labelled promoter DNA in EMSA binding buffer {20 mM HEPES, pH 7.6, containing 30 mM KCl, 5 mM $(NH_4)_2SO_4$, 1 mM EDTA, 1 mM DTT, 0.2 % (w/v) Tween 20 and 5 µg ml^{-1} poly[d(I-C)]}. The reaction was incubated at room temperature for 45 min, and samples were then separated by

electrophoresis on a 6 % native polyacrylamide gel and visualized on an Odyssey Infrared Imaging System (Li-COR Biosciences). Control binding reactions were performed with extracts from *E. coli* BL21-CodonPlusBL21(DE3)-RIPL cells harbouring the pET28a vector control. A non-specific DNA fragment was amplified from the *PA4881* promoter region using DY-682 IR-labelled primers pF81emsa and pR81emsa, and served as negative DNA-binding controls in the EMSA.

Bioinformatic analysis. The PA4354 protein sequence was aligned with several other ArsR/SmtB-family regulators, including ArsR (NP_417958.1), SmtB (P30340.1), NmtR (NP_218261.1), CzrA (O31844.1), CadC (ZP_03565990.1), KmtR (NP_215342.1), SdpR (NP_391259.1), PigS (CBY83976.1), NolR (CAA41777.1), HlyU (NP_230327.1), BigR (Q8UAA8.3), YgaV (NP_417153.1), CmtR (NP_216510.1) and CyeR (NP_602237.1), using MAFFT version 6, and the resulting alignment was analysed and edited using BioEdit (Hall, 1999; Katoh & Toh, 2008). To determine whether PA4354 and homologous repressors exhibited conserved autoregulatory binding sites in their promoters, the upstream regions of 57 putative PA4354 orthologues were retrieved from the Database of Prokaryotic Operons (DOOR) and analysed for the presence of conserved motifs (Mao *et al.*, 2009). Upstream sequences of approximately 200 bp retrieved from each identified PA4354-like regulator were searched using the Multiple Em for Motif Elicitation (MEME) algorithm for the presence of conserved motifs using the following parameters: motif occurrence, one per sequence; $\geqslant$6 optimum motif width $\leqslant$50 (Bailey & Elkan, 1994). To determine the distribution of this putative PA4354 binding motif in the PAO1 genome the Motif Alignment and Search Tool (MAST) was employed (Bailey & Gribskov, 1998).

RESULTS

PA4354 (PyeR) encodes a novel, non-classical member of the ArsR family

PA4354 is predicted to be an ArsR-family transcriptional repressor, as it contains the conserved helix–turn–helix domain found in ArsR-family regulators in its primary sequence. However, PA4354 does not harbour any of the previously characterized metal(loid)-binding sequence motifs associated with classical ArsR regulators, as determined by bioinformatic analysis using the ExPASy search tool (Campbell *et al.*, 2007; Osman & Cavet, 2010). Moreover, it exhibits a unique 13 amino acid region in its primary sequence, which does not align with previously characterized ArsR-family repressors and distinguishes PA4354 from other ArsR repressors (Fig. 1). Orthologues of PA4354, containing the non-classical features, are found in many micro-organisms among diverse bacterial genera, including *Pseudomonas*, *Rhizobium*, *Bordetella* and *Burkholderia*.

To further investigate whether PA4354 is a metal(loid)-responsive regulator, we examined if diverse metal(loid)s [including $ZnSO_4$, V_2SO_4, $MnCl_2$, MoO_4Na_2, $NaAsO_2$, CdCl, $CuSO_4$, K_2TeO_3, $CoCl_2$, $NiCl_2$, $FeCl_3$, $CrCl_3$, $C_8H_4K_2O_{12}Sb_2$, $AgNO_3$, $Pb(NO_3)_2$, $AuCl_3$, $BiNO_3$, Na_2O_3Se and $HgCl_2$] could induce *PA4354*. For this, a pMP-PA4354p vector,

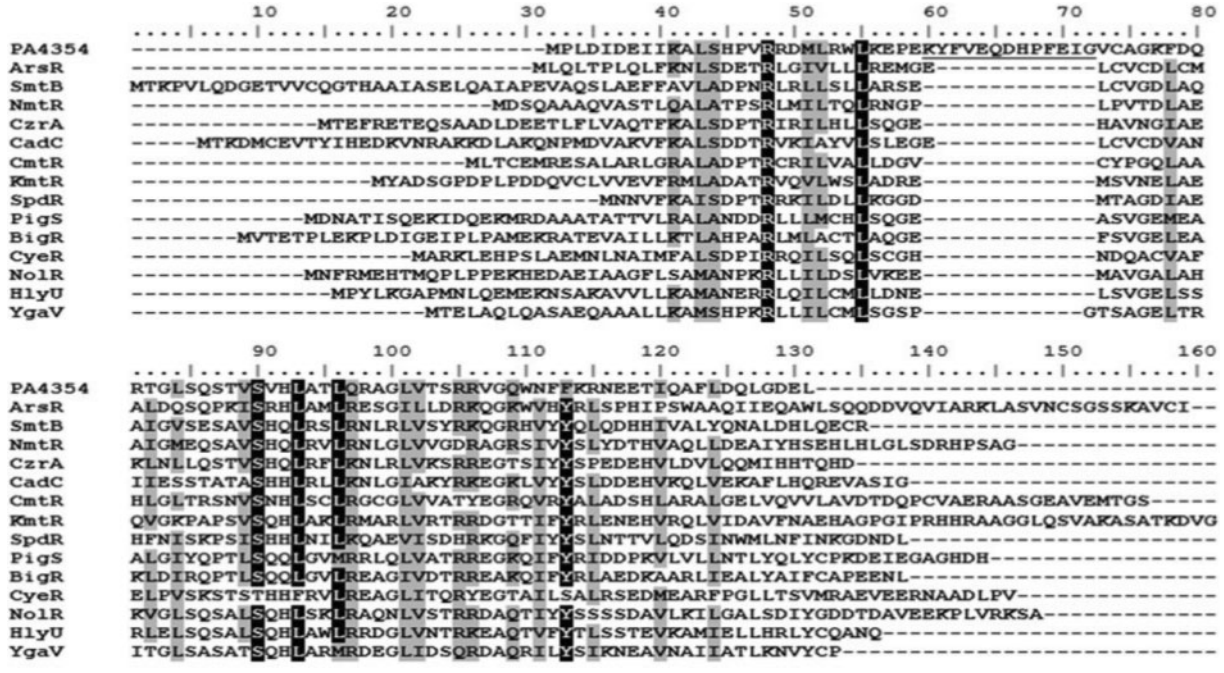

Fig. 1. Alignment of PyeR with diverse ArsR-family repressors. PyeR exhibits atypical sequence in its N-terminal region (underlined), which does not align with other characterized ArsR-family repressors and precedes the only cysteine residue of PyeR. Conserved residues in the alignment are highlighted (black, >80 % identical residues; grey, >80 % similar residues).

which contains the *PA4354*-promoter region upstream of a promoterless *lacZ*-reporter plasmid, was used (Tian *et al.*, 2009a). Approximately 50 % of the metals inhibited growth of *P. aeruginosa* (Table S1). Interestingly, *PA4354* expression was induced in the presence of lead and tellurite, but not by the other metals tested (Table S1). However, this induction was apparently independent of *PA4354*, as disruption of *PA4354* did not abrogate the observed differential changes. This suggests that although lead and tellurite positively influence expression from the *PA4354* promoter, they are not cognate metal(loid) inducers of PA4354 in the classical sense of the direct binding and de-repression observed for metal(loid)-responsive ArsR repressors. Moreover, tellurite also inhibited the growth of *P. aeruginosa*, suggesting that it would induce *PA4354* expression at a sub-inhibitory concentration. In addition, deletion of *PA4354* had no impact on the level of resistance to inducing metal(loid)s, as the MIC levels of lead and tellurite, 0.125 and 0.06 mM, respectively, were unchanged upon deletion of *PA4354*. This is not surprising, as PA4354 is encoded within a putative operon with an uncharacterized MFS transporter and the OYE-family reductase XenB, and not with metal(loid) resistance genes, unlike classical members of the metal-responsive ArsR family (Pak *et al.*, 2000; van Dillewijn *et al.*, 2008).

Given that PA4354 is located in a putative operon with the OYE protein *xenB* we propose the gene name PyeR (*Pseudomonas* yellow enzyme regulator) for PA4354, in accordance with the study of Ehira *et al.* (2010), where an ArsR-family repressor was observed to regulate expression of an OYE-family enzyme in *Corynebacterium glutamicum*. By extension, the MFS transporter PA4355 was named PyeM (*Pseudomonas* yellow enzyme MFS transporter). Hereafter, PA4354 and PA4355 are referred to as PyeR and PyeM, respectively. Comparative analysis of PyeR orthologues revealed that many ArsR-family regulators (COG0640) are also associated with MFS transporters (COG0477) and OYE-family enzymes (COG1907). This is reflected by a strong association score between COG0640 and both COG0477 (0.824) and COG1902 (0.671) in the STRING database (Szklarczyk *et al.*, 2011). This suggests the existence of a subgroup of ArsR-family repressors with homology to PyeR that regulate expression of MFS transporters and OYE-family enzymes, as opposed to classical ArsR-family regulators, which regulate expression of genes associated with metal(loid) resistance (e.g. COG0798, COG1393, COG1230).

PyeR has autoregulatory properties

As both classical and non-classical ArsR-family repressors generally function as autoregulatory proteins (Busenlehner *et al.*, 2003), expression analysis of *PyeR* was performed to investigate the autoregulatory characteristics of PyeR. For this, the pMP-PA4354p vector, which contains the *pyeR*-promoter region upstream of a promoterless *lacZ*-reporter plasmid, was used. Expression of *pyeR* in PAO1 wild-type reached 395.3 ± 19.4 Miller units (mean $\pm$ SD) during exponential growth (absorbance of 0.6–0.8 at 600 nm, equivalent to ~4 h of growth with a starting OD_{600} of 0.02). By contrast, expression of the vector control (pMP190) over all conditions was 20.27 ± 11.04 Miller units. Overexpression of PyeR (pME6032-PA4354) resulted in repression of *pyeR* promoter activity, demonstrating that PyeR functions as an autorepressor (Fig. 2). In addition, *pyeR* promoter activity was elevated in a *pyeR* deletion mutant compared with wild-type cells and on overexpression of its known transcriptional activator MexT, which further substantiates the evidence that PyeR has autoregulatory properties (Table 3).

Identification of the PyeR autoregulatory motif

As orthologues of PyeR are present in diverse species, these sequences could be used to identify the putative autoregulatory site of PyeR. Upstream regions of PyeR orthologues were retrieved from the DOOR database (Mao *et al.*, 2009). These sequences were aligned and searched for the presence of a conserved motif using the MEME algorithm (Bailey & Elkan, 1994). This identified a putative PyeR autoregulatory site which was highly conserved among all 57 retrieved upstream regions of PyeR orthologues. The putative PyeR binding motif was located downstream of the previously identified MexT binding site and overlaps a putative −10 region (Fig. 3). Apart from the upstream region of *pyeR*, no highly significant hits to the putative PyeR binding motif were identified within the PAO1 genome using the MAST algorithm, suggesting that this motif is not conserved outside the PyeR promoter region (Bailey & Gribskov, 1998).

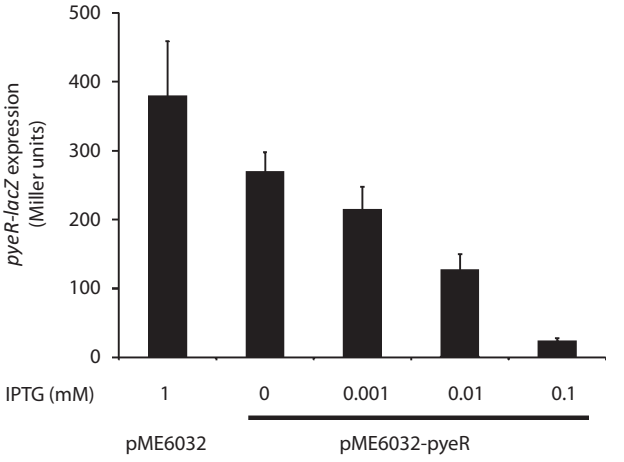

Fig. 2. PyeR has autoregulatory properties. Induction of *pyeR* expression from the pMP-PA4354p promoter–*lacZ* fusion was determined in the presence of the PyeR overexpression construct pME6032-PA4354. Increasing concentrations of IPTG led to increased PyeR and resulted in decreased expression from the *pyeR* promoter. Data shown are mean values of three biological experiments; error bars, SD.

Table 3. Influence of *pyeR* deletion and *mexT* overexpression on *pyeR* promoter activity

Values are mean ± SD of three independent biological replicates.

Plasmid	Exponential*		Stationary†	
	PAO1 WT	PAO1Δ*PA4354*	PAO1 WT	PAO1Δ*PA4354*
pME6032	295 ± 54	468 ± 70	116 ± 9	154 ± 27
pME6032-mexT	1560 ± 188	2572 ± 33	560 ± 26	881 ± 75

*Observed β-galactosidase activity in exponential phase cultures (OD_{600} 0.4–0.7).
†Observed β-galactosidase activity in stationary phase cultures (OD_{600} >2.5, samples taken at 24 h).

However, the absence of this motif does not rule out the possibility that PyeR binds to other motifs. Further analysis will be required to investigate this; for example, microarray analysis on a wild-type and *pyeR* mutant strain under the conditions in which PyeR exerts its own autoregulation.

To confirm the role of the identified PyeR binding motif in PyeR autorepression, site-directed mutagenesis of this region was performed. Mutation of conserved residues within the putative *pyeR* autoregulatory site (TATGC-N_8-CGATA-N_5-TCG-N_8-CGA) resulted in increased expression from the *pyeR* promoter in the presence of the *pyeR* overexpressor (pME6032-PA4354) (Fig. 4). This demonstrated the importance of the identified *cis*-acting regulatory site in mediating *PyeR* autorepression.

PyeR binds directly to its own upstream promoter region

EMSA was used to demonstrate unequivocally that PyeR binds directly to its own promoter. A His-tagged PyeR expression construct was generated (pET28a-*pyeR*H6C) and the PyeR repressor was subsequently purified by nickel affinity column chromatography. As expected, the purified PyeR protein caused a mobility shift in the presence of an IR-labelled DNA probe spanning the *PA4353-pyeR* intergenic region (Fig. 5). In contrast, no shift was observed in the presence of a non-specific DNA probe amplified from the *PA4881* upstream region, which does not contain a PyeR autoregulatory motif (Fig. 5). This demonstrates the direct and specific binding of PyeR to its own upstream promoter region, consistent with the autoregulatory function of the PyeR autorepressor.

pyeR is co-transcribed with *pyeM* and *xenB*

To investigate whether the predicted *pyeR-pyeM-xenB* operon was expressed as a tri-cistronic transcript, RT-PCR was employed to determine the nature of the RNA transcript(s). For this, cDNA was synthesized from RNA isolated from PAO1 (pME6032-mexT), which harbours a MexT overexpression construct to drive induction of *pyeR-pyeM-xenB*. Primers flanking the intergenic regions between *pyeR* and *pyeM* as well as between *pyeM* and *xenB* were used to verify that the tri-cistronic transcript was expressed. Amplification of the *pyeR-pyeM* and *pyeM-xenB* intergenic regions from reverse-transcribed cDNA confirmed the co-transcription of *pyeR*, *pyeM* and *xenB* (Fig. 6).

The *pyeR-pyeM-xenB* operon exhibits complex regulation

PyeR has previously been demonstrated to be directly regulated by MexT, which has been shown to regulate key

Fig. 3. A highly conserved motif was identified in the promoter region of the PyeR repressor. This motif was present downstream of the MexT binding site. Putative *pyeR* −35 and −10 sites are indicated by broken lines. A motif logo illustrating a position-specific scoring matrix for the PyeR binding site is illustrated above the matching nucleotide sequence in the *pyeR* upstream region. Highly conserved nucleotides are highlighted in grey and the nucleotides of the *nod* boxes within the MexT binding site are boxed. Conserved nucleotides within the PyeR binding motif which were subsequently targeted for site-directed mutagenesis are indicated by black dots.

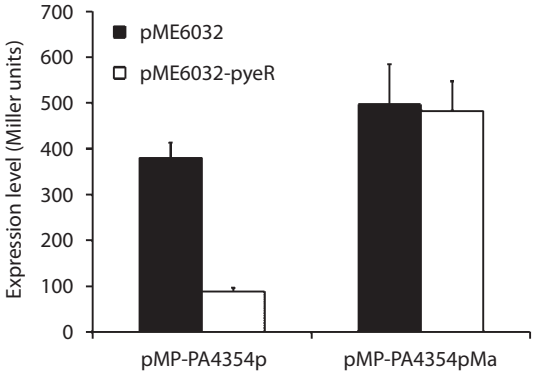

Fig. 4. Validation of the PyeR binding site by site-directed mutagenesis. An AT–GC change was introduced into the conserved nucleotides of the putative PyeR binding motif (indicated in Fig. 5). The mutated *pyeR* promoter region was cloned into pMP190 to yield the mutated promoter fusion pMP-PA4354pMa. Overexpression of PyeR (white bars) repressed promoter activity from pMP-PA4354p compared with the empty vector control (black bars) but not from the mutated promoter in pMP-PA4354pMa in the presence of 1 μM IPTG, which induces expression of PyeR. Expression levels of the empty pMP190 vector were only 17.38 ± 7.8 and 18.82 ± 13.07, respectively. Data shown are mean values of three biological experiments; error bars, SD.

pathogenic traits in *P. aeruginosa*, such as biofilm formation, expression of the type III secretion system, phenazine production and antibiotic resistance (Tian *et al.*, 2009a, b). As *pyeR* promoter activity is observed in wild-type cells, in which MexT is not expressed, it is likely that other regulatory proteins are also involved in the regulation of *pyeR* (Tian *et al.*, 2009b). To investigate this further, the

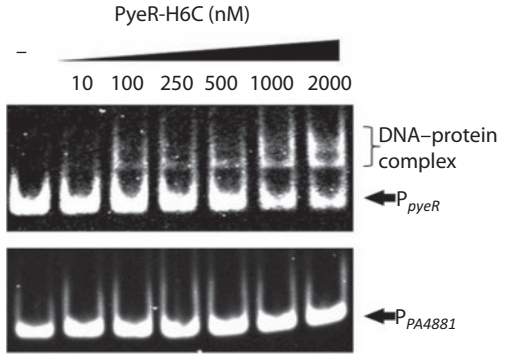

Fig. 5. Direct binding of PyeR to the *pyeR* upstream region. His-tag-purified PyeR causes a mobility shift in the presence of the *pyeR* upstream region (top row). No shift was observed with a non-specific DNA target amplified from the *PA4881* upstream region which lacks the PyeR binding site. The concentration of His-tagged PyeR used in each assay is indicated above the gel image.

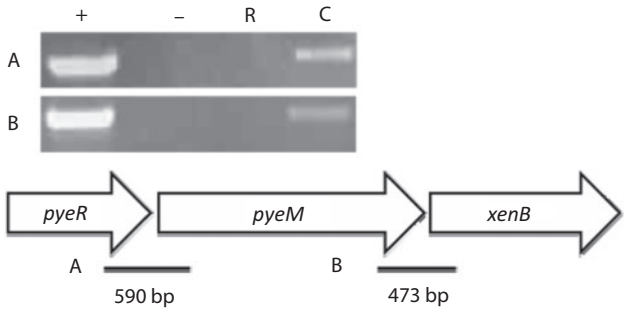

Fig. 6. Confirmation of the *pyeR-pyeM-xenB* operon structure by RT-PCR. +, Positive control (PAO1 gDNA); –, negative control (cDNA synthesis reaction mixture to which no template was added); R, DNase-treated RNA isolated from PAO1(pME6032-mexT) before cDNA synthesis; C, cDNA synthesized from RNA isolated from PAO1(pME6032-mexT) using a specific primer complementary to the 3′ end of the *xenB* transcript. The regions amplified in images A and B are indicated by solid black lines in the diagram of the *pyeR-pyeM-xenB* operon structure below the gel images.

expression of *pyeR* in a MexT deletion background was assessed. Deletion of MexT had no impact on *pyeR* promoter activity (256 ± 30 Miller units) in PAO1 as the expression level was comparable with PAO1 wild-type (287 ± 15 Miller units), implicating other regulators in the modulation of *pyeR* expression. Furthermore, expression of *pyeR* declined to approximately 80 Miller units in stationary phase, whereas the empty vector control (pMP190) did not reach above 60 Miller units at any time point, with a mean over all time points of 15.97 ± 14.22 Miller units (Fig. 7). This stationary phase repression occurred irrespective of whether *pyeR* was deleted or whether MexT was over-expressed, ruling out a role for either regulator in *pyeR* downregulation during stationary phase (Table 3). This further suggests that other regulatory elements are involved in the regulation of *pyeR*, which may integrate this regulator into several signal transduction pathways. Further research will focus on the elucidation of other elements that are involved in the regulation of *pyeR*.

PyeR plays a role in biofilm formation

As PyeR is a direct regulatory target of MexT, which downregulates several virulence-related phenotypes, we hypothesized that the PyeR repressor might influence MexT-linked phenotypes. Neither deletion of *pyeR* nor overexpression of *pyeR* had any impact on antibiotic resistance or virulence-related phenotypes, including expression of the type III secretion system, pyocyanin production and early attachment (data not shown). However, flow cell biofilm experiments showed that the architecture of 3-day-old biofilms of the *pyeR* mutant differed significantly from that of PAO1 wild-type (Fig. 8). The mushroom-shaped microcolony structures were larger and more abundant in

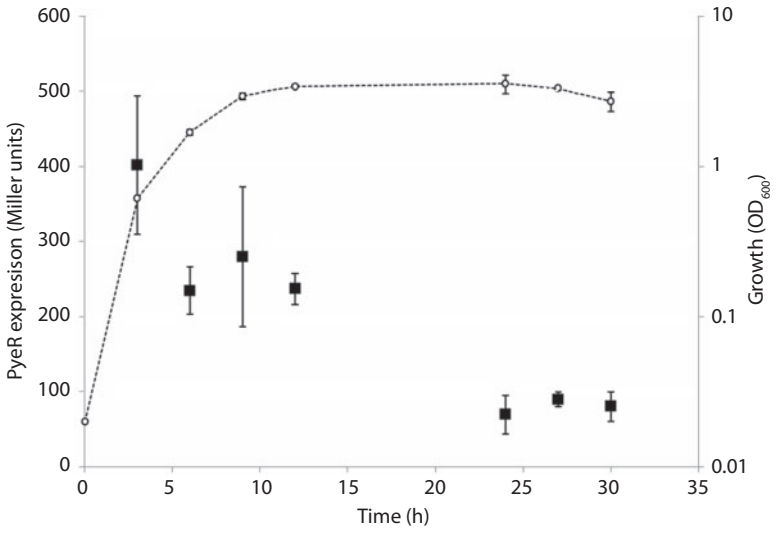

Fig. 7. PyeR expression is induced in exponential phase and declines at higher cell densities. ■, Expression from the pMP-PA4354p *lacZ* reporter fusion (primary axis) measured in Miller units. ○, Growth of PAO1 harbouring pMP-PA4354p represented by log(OD_{600}) at each time point (secondary axis). Data shown are mean values of three biological experiments; error bars, SD.

the mutant compared with the wild-type biofilm (Fig. 8). To investigate whether PyeM and/or XenB are also involved in biofilm formation, a *pyeM* out-of-frame deletion mutant was constructed that resulted in loss of both *pyeM* and *xenB* transcript. Flow cell experiments showed that there was no difference in biofilm architecture between PAO1 wild-type and this mutant (data not shown), suggesting that only PyeR plays a role in biofilm formation.

To assess further the role of PyeR in biofilm formation, a tight microcolony assay was performed. Deletion of *pyeR* resulted in loss of tight microcolony formation in ASM (Fig. S1a, b). This phenotype was restored by complementation with a plasmid expressing *pyeR in trans* (Fig. S1c, d). Moreover, a similar phenotype was observed in another *P. aeruginosa* model strain, PA14, as a mutant with a mariner transposon in *PA4354* (PA14 *PA4354*::*Tm*) (Liberati *et al.*, 2006) was unable to form a tight microcolony (Fig. S1d, e). Taking the above data together, PyeR is implicated in biofilm formation, which provides a novel function for this non-classical ArsR-family transcriptional regulator.

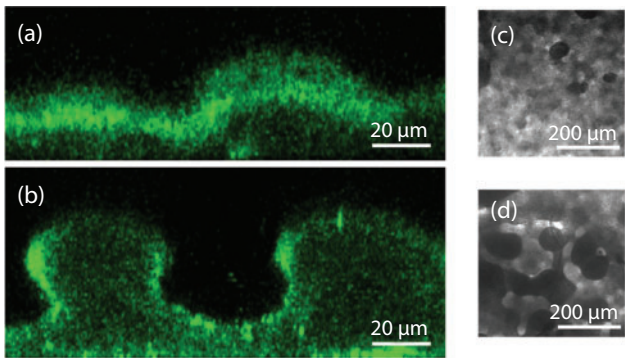

Fig. 8. Modulated 3-day-old biofilm architecture. Visual representation of biofilm stained with SYTO 9 using a confocal scanning microscope. (a, b) Side views of a *z*-stack analysis; (c, d) bright-field overview images. (a, c) PAO1 wild-type pME6032; (b, d) PAO1Δ*PA4354* pME6032. Images shown are representative of three independent biological replicates. Bars: (a, b) 20 µm; (c, d) 200 µm.

DISCUSSION

PyeR is a novel ArsR-type transcriptional regulator from *P. aeruginosa*, which exhibits classical features such as a conserved helix–turn–helix domain, negative autoregulation and transcription as part of an operon. However, it does not exhibit metal(loid) perception or resistance characteristics associated with classical ArsR-family regulators. This is an emerging theme within the ArsR family, where several members have now been demonstrated to be involved in processes unrelated to metal(loid) perception or resistance (Ehira *et al.*, 2010; Ellermeier *et al.*, 2006; Gristwood *et al.*, 2011; Gueuné *et al.*, 2008; Guimarães *et al.*, 2011). For example, the SdpR repressor of *Bacillus subtilis*, which regulates cannibalistic behaviour during sporulation, dissociates from its promoter via sequestration at the cell membrane by a cell membrane immunity protein (Ellermeier *et al.*, 2006). The HlyU repressor of *Vibrio vulnificus* activates expression of its target by acting as an antirepressor of a histone-like nucleoid structuring protein, which negatively regulates expression of the *rtxA1* toxin-encoding gene (Liu *et al.*, 2009). As such, PyeR belongs to a growing subgroup of the non-classical ArsR family of transcriptional regulators linked to diverse physiological phenotypes rather than specifically to metal resistance.

The ArsR-family repressor CyeR of *Corynebacterium glutamicum* has been shown to be induced by oxidative and thiol-specific stress rather than the presence of metals and also regulates the OYE-family enzyme Cye1, which has

homology to XenB (Ehira *et al.*, 2010). This is interesting, as the two metals that were found to induce expression of *pyeR-pyeM-xenB* are implicated in oxidative stress. Moreover, transcriptome analysis has shown upregulation of *pyeR* transcript in response to hydrogen peroxide (Palma *et al.*, 2004). Tellurium has been shown to induce a thiol-specific stress response in *Pseudomonas pseudoalcaligenes*, and the pathotoxicity of lead to eukaryotic organisms is attributed to toxicity-induced oxidative stress (Tremaroli *et al.*, 2009; Verstraeten *et al.*, 2008). As metal(loid)-mediated induction of expression from the *pyeR* promoter was observed in both *mexT* and *pyeR* deletion backgrounds, it is likely that the *pyeR-pyeM-xenB* operon is regulated by another unidentified regulator in response to metal(loid)-induced changes in the cellular redox environment, independently of both MexT and PyeR.

Although XenB is known to catalyse the reductive removal of nitro groups from electrophilic pollutants, including 2,4,6-trinitrotoluene and nitroglycerine, these are unlikely to reflect the natural substrates of XenB (Pak *et al.*, 2000). As a member of the OYE family, XenB is likely to be involved in the reduction of α,β-unsaturated carbonyl compounds, which may emerge from metabolism or be encountered in the environment (Breithaupt *et al.*, 2009; Trotter *et al.*, 2006; Williams & Bruce, 2002). The fact that *pyeR* promoter activity is observed in exponentially growing cells suggests that the substrate(s) of the *pyeR-pyeM-xenB* operon are compounds endogenous to *P. aeruginosa*. Such molecules or their breakdown products could represent the specific ligands recognized by PyeR. Thus, it now appears probable that several ArsR-family regulators modulate gene expression in response to non-metalloid inducing molecules. However, formal validation of this hypothesis awaits the identification of the first non-metalloid ArsR-binding ligand. Just as work on metal(loid)-perceptive ArsR regulators has allowed the identification of motifs associated with specific metal(-loid)s, the identification of non-metal(loid) ligands would greatly increase our understanding of ArsR-family repressor ligand interactions. PyeR lacks any previously determined metal-binding motifs in its protein sequence and appears not to play a direct role in metal perception, although the identified unique 13 amino acid region in PyeR (and its many orthologues) may have significance in defining the interaction of PyeR with a non-metal(loid) ligand.

Although non-classical ArsR-family transcriptional regulators are linked to many physiological processes, this study is believed to be only the second report to implicate the ArsR family of transcriptional regulators in biofilm formation. The BigR repressor of *Xylella fastidiosa* and *Agrobacterium tumifaciens* has been shown to negatively influence biofilm formation and the expression of genes involved in hydrogen sulphide resistance (Barbosa & Benedetti, 2007). Similarly to PyeR, deletion of the BigR target gene, *bhl*, had no effect on biofilm formation (Barbosa & Benedetti, 2007; Guimarães *et al.*, 2011). This may be due to functional redundancy and interplay among biofilm-associated genes or to regulatory effects of BigR on as-yet-unidentified targets, as may also be the case for PyeR. The high-throughput biofilm screen in which PyeR was independently identified was performed in ASM. This medium closely resembles the sputum found in the lungs of cystic fibrosis patients, in whom *P. aeruginosa* is the main cause of morbidity and mortality (Sriramulu *et al.*, 2005). As PyeR is essential for tight microcolony formation in this medium, this indicates that PyeR might be a key player in biofilm formation *in vivo*.

ACKNOWLEDGEMENTS

We thank Pat Higgins for excellent technical assistance during the course of this work. We thank Dr Jerry Reen for discussions and critical reading of the manuscript. This research was supported in part by grants awarded by the European Commission (FP7-KBBE-2012-6, CP-TP-312184; FP7-KBBE-2012-6, 311975; OCEAN.2011-2, 287589; MTKD-CT-2006-042062, O36314), Science Foundation Ireland (SFI 07/IN.1/B948; 08/RFP/GEN1295; 08/RFP/GEN1319; 09/RFP/BMT2350), the Department of Agriculture and Food (DAF RSF 06 321; DAF RSF 06 377; FIRM 08/RDC/629), the Irish Research Council for Science, Engineering and Technology (RS/2010/2413; 05/EDIV/FP107), the Health Research Board (RP/2006/271; RP/2007/290; HRA/2009/146), the Environmental Protection Agency (EPA2006-PhD-S-21; EPA2008-PhD-S-2), the Marine Institute (Beaufort award C2CRA 2007/082) and the Higher Education Authority of Ireland (PRTLI3; PRTLI4).

REFERENCES

Arunkumar, A. I., Campanello, G. C. & Giedroc, D. P. (2009). Solution structure of a paradigm ArsR family zinc sensor in the DNA-bound state. *Proc Natl Acad Sci U S A* **106**, 18177–18182.

Bailey, T. L. & Elkan, C. (1994). Fitting a mixture model by expectation maximization to discover motifs in biopolymers. *Proc Int Conf Intell Syst Mol Biol* **2**, 28–36.

Bailey, T. L. & Gribskov, M. (1998). Combining evidence using p-values: application to sequence homology searches. *Bioinformatics* **14**, 48–54.

Barbosa, R. L. & Benedetti, C. E. (2007). BigR, a transcriptional repressor from plant-associated bacteria, regulates an operon implicated in biofilm growth. *J Bacteriol* **189**, 6185–6194.

Breithaupt, C., Kurzbauer, R., Schaller, F., Stintzi, A., Schaller, A., Huber, R., Macheroux, P. & Clausen, T. (2009). Structural basis of substrate specificity of plant 12-oxophytodienoate reductases. *J Mol Biol* **392**, 1266–1277.

Busenlehner, L. S., Pennella, M. A. & Giedroc, D. P. (2003). The SmtB/ArsR family of metalloregulatory transcriptional repressors: structural insights into prokaryotic metal resistance. *FEMS Microbiol Rev* **27**, 131–143.

Cai, J., Salmon, K. & DuBow, M. S. (1998). A chromosomal *ars* operon homologue of *Pseudomonas aeruginosa* confers increased resistance to arsenic and antimony in *Escherichia coli*. *Microbiology* **144**, 2705–2713.

Campbell, D. R., Chapman, K. E., Waldron, K. J., Tottey, S., Kendall, S., Cavallaro, G., Andreini, C., Hinds, J., Stoker, N. G. & other authors (2007). Mycobacterial cells have dual nickel-cobalt sensors: sequence relationships and metal sites of metal-responsive repressors are not congruent. *J Biol Chem* **282**, 32298–32310.

Ehira, S., Teramoto, H., Inui, M. & Yukawa, H. (2010). A novel redox-sensing transcriptional regulator CyeR controls expression of an Old Yellow Enzyme family protein in *Corynebacterium glutamicum*. *Microbiology* **156**, 1335–1341.

Ellermeier, C. D., Hobbs, E. C., Gonzalez-Pastor, J. E. & Losick, R. (2006). A three-protein signaling pathway governing immunity to a bacterial cannibalism toxin. *Cell* **124**, 549–559.

Fisher, C. L. & Pei, G. K. (1997). Modification of a PCR-based site-directed mutagenesis method. *Biotechniques* **23**, 570–571, 574.

Gristwood, T., McNeil, M. B., Clulow, J. S., Salmond, G. P. & Fineran, P. C. (2011). PigS and PigP regulate prodigiosin biosynthesis in *Serratia* via differential control of divergent operons, which include predicted transporters of sulfur-containing molecules. *J Bacteriol* **193**, 1076–1085.

Gueuné, H., Durand, M. J., Thouand, G. & DuBow, M. S. (2008). The *ygaVP* genes of *Escherichia coli* form a tributyltin-inducible operon. *Appl Environ Microbiol* **74**, 1954–1958.

Guimarães, B. G., Barbosa, R. L., Soprano, A. S., Campos, B. M., de Souza, T. A., Tonoli, C. C., Leme, A. F., Murakami, M. T. & Benedetti, C. E. (2011). Plant pathogenic bacteria utilize biofilm growth-associated repressor (BigR), a novel winged-helix redox switch, to control hydrogen sulfide detoxification under hypoxia. *J Biol Chem* **286**, 26148–26157.

Hall, T. A. (1999). BioEdit: a user-friendly biological sequence alignment editor and analysis program for Windows 95/98/NT. *Nucleic Acids Symp Ser* **41**, 95–98.

Harvie, D. R., Andreini, C., Cavallaro, G., Meng, W., Connolly, B. A., Yoshida, K., Fujita, Y., Harwood, C. R., Radford, D. S. & other authors (2006). Predicting metals sensed by ArsR-SmtB repressors: allosteric interference by a non-effector metal. *Mol Microbiol* **59**, 1341–1356.

Heeb, S., Itoh, Y., Nishijyo, T., Schnider, U., Keel, C., Wade, J., Walsh, U., O'Gara, F. & Haas, D. (2000). Small, stable shuttle vectors based on the minimal pVS1 replicon for use in Gram-negative, plant-associated bacteria. *Mol Plant Microbe Interact* **13**, 232–237.

Hoang, T. T., Karkhoff-Schweizer, R. R., Kutchma, A. J. & Schweizer, H. P. (1998). A broad-host-range Flp-FRT recombination system for site-specific excision of chromosomally-located DNA sequences: application for isolation of unmarked *Pseudomonas aeruginosa* mutants. *Gene* **212**, 77–86.

Huckle, J. W., Morby, A. P., Turner, J. S. & Robinson, N. J. (1993). Isolation of a prokaryotic metallothionein locus and analysis of transcriptional control by trace metal ions. *Mol Microbiol* **7**, 177–187.

Janga, S. C. & Pérez-Rueda, E. (2009). Plasticity of transcriptional machinery in bacteria is increased by the repertoire of regulatory families. *Comput Biol Chem* **33**, 261–268.

Katoh, K. & Toh, H. (2008). Recent developments in the MAFFT multiple sequence alignment program. *Brief Bioinform* **9**, 286–298.

Liberati, N. T., Urbach, J. M., Miyata, S., Lee, D. G., Drenkard, E., Wu, G., Villanueva, J., Wei, T. & Ausubel, F. M. (2006). An ordered, nonredundant library of *Pseudomonas aeruginosa* strain PA14 transposon insertion mutants. *Proc Natl Acad Sci U S A* **103**, 2833–2838.

Liu, M., Naka, H. & Crosa, J. H. (2009). HlyU acts as an H-NS antirepressor in the regulation of the RTX toxin gene essential for the virulence of the human pathogen *Vibrio vulnificus* CMCP6. *Mol Microbiol* **72**, 491–505.

Mao, F., Dam, P., Chou, J., Olman, V. & Xu, Y. (2009). DOOR: a database for prokaryotic operons. *Nucleic Acids Res* **37** (Database issue), D459–D463.

Mignot, T., Mock, M. & Fouet, A. (2003). A plasmid-encoded regulator couples the synthesis of toxins and surface structures in *Bacillus anthracis*. *Mol Microbiol* **47**, 917–927.

Miller, J. H. (1972). *Experiments in Molecular Genetics*. Cold Spring Harbor, NY: Cold Spring Harbor Laboratory.

Osman, D. & Cavet, J. S. (2010). Bacterial metal-sensing proteins exemplified by ArsR-SmtB family repressors. *Nat Prod Rep* **27**, 668–680.

Pak, J. W., Knoke, K. L., Noguera, D. R., Fox, B. G. & Chambliss, G. H. (2000). Transformation of 2,4,6-trinitrotoluene by purified xenobiotic reductase B from *Pseudomonas fluorescens* I-C. *Appl Environ Microbiol* **66**, 4742–4750.

Palma, M., DeLuca, D., Worgall, S. & Quadri, L. E. (2004). Transcriptome analysis of the response of *Pseudomonas aeruginosa* to hydrogen peroxide. *J Bacteriol* **186**, 248–252.

Pamp, S. J., Gjermansen, M., Johansen, H. K. & Tolker-Nielsen, T. (2008). Tolerance to the antimicrobial peptide colistin in *Pseudomonas aeruginosa* biofilms is linked to metabolically active cells, and depends on the *pmr* and *mexAB-oprM* genes. *Mol Microbiol* **68**, 223–240.

Sambrook, J. (2001). *Molecular Cloning: a Laboratory Manual*. Cold Spring Harbor, NY: Cold Spring Harbor Laboratory.

San Francisco, M. J., Hope, C. L., Owolabi, J. B., Tisa, L. S. & Rosen, B. P. (1990). Identification of the metalloregulatory element of the plasmid-encoded arsenical resistance operon. *Nucleic Acids Res* **18**, 619–624.

Shi, W., Dong, J., Scott, R. A., Ksenzenko, M. Y. & Rosen, B. P. (1996). The role of arsenic-thiol interactions in metalloregulation of the *ars* operon. *J Biol Chem* **271**, 9291–9297.

Simon, R., Priefer, U. & Pühler, A. (1983). A broad host range mobilization system for *in vivo* genetic engineering: transposon mutagenesis in Gram negative bacteria. *Biotechnology* **1**, 784–791.

Spaink, H. P., Okker, R. J. H., Wijffelman, C. A., Pees, E. & Lugtenberg, B. J. J. (1987). Promoters in the nodulation region of the *Rhizobium leguminosarum* Sym plasmid pRL1J1. *Plant Mol Biol* **9**, 27–39.

Sriramulu, D. D., Lünsdorf, H., Lam, J. S. & Römling, U. (2005). Microcolony formation: a novel biofilm model of *Pseudomonas aeruginosa* for the cystic fibrosis lung. *J Med Microbiol* **54**, 667–676.

Stover, C. K., Pham, X. Q., Erwin, A. L., Mizoguchi, S. D., Warrener, P., Hickey, M. J., Brinkman, F. S., Hufnagle, W. O., Kowalik, D. J. & other authors (2000). Complete genome sequence of *Pseudomonas aeruginosa* PAO1, an opportunistic pathogen. *Nature* **406**, 959–964.

Summers, A. O. (2009). Damage control: regulating defenses against toxic metals and metalloids. *Curr Opin Microbiol* **12**, 138–144.

Szklarczyk, D., Franceschini, A., Kuhn, M., Simonovic, M., Roth, A., Minguez, P., Doerks, T., Stark, M., Muller, J. & other authors (2011). The STRING database in 2011: functional interaction networks of proteins, globally integrated and scored. *Nucleic Acids Res* **39** (Database issue), D561–D568.

Tian, Z. X., Fargier, E., Mac Aogáin, M., Adams, C., Wang, Y. P. & O'Gara, F. (2009a). Transcriptome profiling defines a novel regulon modulated by the LysR-type transcriptional regulator MexT in *Pseudomonas aeruginosa*. *Nucleic Acids Res* **37**, 7546–7559.

Tian, Z. X., Mac Aogáin, M., O'Connor, H. F., Fargier, E., Mooij, M. J., Adams, C., Wang, Y. P. & O'Gara, F. (2009b). MexT modulates virulence determinants in *Pseudomonas aeruginosa* independent of the MexEF-OprN efflux pump. *Microb Pathog* **47**, 237–241.

Tremaroli, V., Workentine, M. L., Weljie, A. M., Vogel, H. J., Ceri, H., Viti, C., Tatti, E., Zhang, P., Hynes, A. P. & other authors (2009). Metabolomic investigation of the bacterial response to a metal challenge. *Appl Environ Microbiol* **75**, 719–728.

Trotter, E. W., Collinson, E. J., Dawes, I. W. & Grant, C. M. (2006). Old yellow enzymes protect against acrolein toxicity in the yeast *Saccharomyces cerevisiae*. *Appl Environ Microbiol* **72**, 4885–4892.

van Dillewijn, P., Wittich, R. M., Caballero, A. & Ramos, J. L. (2008). Subfunctionality of hydride transferases of the old yellow enzyme family of flavoproteins of *Pseudomonas putida*. *Appl Environ Microbiol* **74**, 6703–6708.

Verstraeten, S. V., Aimo, L. & Oteiza, P. I. (2008). Aluminium and lead: molecular mechanisms of brain toxicity. *Arch Toxicol* **82**, 789–802.

Williams, R. E. & Bruce, N. C. (2002). 'New uses for an Old Enzyme' – the Old Yellow Enzyme family of flavoenzymes. *Microbiology* **148**, 1607–1614.

Edited by: W. J. Quax